



TITLE:

Noncontact atomic force microscopy study of copper-phthalocyanines: Submolecular-scale contrasts in topography and energy dissipation

AUTHOR(S):

Fukuma, Takeshi; Kobayashi, Kei; Yamada, Hirofumi; Matsushige, Kazumi

CITATION:

Fukuma, Takeshi ...[et al]. Noncontact atomic force microscopy study of copper-phthalocyanines: Submolecular-scale contrasts in topography and energy dissipation. JOURNAL OF APPLIED PHYSICS 2004, 95(9): 4742-4746

ISSUE DATE:

2004-05-01

URL:

<http://hdl.handle.net/2433/39710>

RIGHT:

Copyright 2004 American Institute of Physics. This article may be downloaded for personal use only. Any other use requires prior permission of the author and the American Institute of Physics.

Noncontact atomic force microscopy study of copper-phthalocyanines: Submolecular-scale contrasts in topography and energy dissipation

Takeshi Fukuma

Department of Electronic Science and Engineering, Kyoto University, Katsura, Nishikyo, Kyoto 615-8510, Japan

Kei Kobayashi

International Innovation Center, Kyoto University, Yoshida-Honmachi, Sakyo, Kyoto 606-8501, Japan

Hirofumi Yamada^{a)} and Kazumi Matsushige

Department of Electronic Science and Engineering, Kyoto University, Katsura, Nishikyo, Kyoto 615-8510, Japan

(Received 12 November 2003; accepted 6 February 2004)

Copper-phthalocyanine (CuPc) thin films on MoS₂ surfaces were investigated by noncontact atomic force microscopy (NC-AFM). Submolecular resolution was successfully obtained in both topographic and dissipation images of CuPc monolayers. For topographic contrasts, the influence of short-range chemical interactions is particularly considered while the dissipation contrasts are discussed in relation to the tip-induced molecular fluctuations. Molecularly-resolved NC-AFM image was also obtained on CuPc multilayer, which revealed the structural difference between the monolayer and multilayer surfaces. The energy dissipation measured on these surfaces showed distinctive difference reflecting the different structural stabilities in the films. Furthermore, local surface modification of CuPc monolayer was demonstrated by NC-AFM. This is a direct evidence for the existence of energy transfer from the vibrating cantilever to the molecules through dissipative tip-sample interactions. © 2004 American Institute of Physics.

[DOI: 10.1063/1.1690485]

I. INTRODUCTION

Noncontact atomic force microscopy (NC-AFM) using the frequency modulation detection method¹ has been shown to be capable of imaging insulating surfaces with true-atomic resolution² as well as conductive surfaces.^{3,4} This capability is particularly important for its applications to organic materials^{5–8} because most of them have poor electrical conductivity. Since the demonstration of the true-atomic resolution in NC-AFM,^{3,4} the imaging mechanism has been intensively studied in both theoretical^{9–11} and experimental^{12,13} aspects. Although its complete understanding has not been achieved yet, it is clear that short-range chemical interactions between a tip front atom and a surface atom play essential roles in the contrast formation.^{12,13} In that sense, organic molecules are useful for studying the imaging mechanism because various molecules with a wide variety of chemical properties are available.

The dissipation process of the cantilever vibration energy during NC-AFM imaging has recently attracted much attention due to the importance for understanding the atomic-scale dynamic behavior taking place at the closest tip approach to the surface and also for future potential applications to atomic- or molecular-manipulations. Dissipation images with true-atomic resolution were first demonstrated in 1997 by Lüthi *et al.*,¹⁴ which evoked a large number of subsequent studies on contrast formation mechanisms in dissipation images.^{15–17} Among them, Gauthier and Tsukada have suggested that the stochastic motion of surface atoms is

one of the important origins of the dissipation. For organic thin films, such structural fluctuation should be more evident because molecules often have loosely-packed or disordered structures and the films are mostly less rigid than inorganic ones.⁷

In this study, we investigated the NC-AFM imaging mechanisms of topography and energy dissipation using copper-phthalocyanine (CuPc) thin films deposited on MoS₂ surfaces. CuPc is a symmetrical macrocyclic compound which consists of four iminoisoindoline units with a copper ion accommodated in the central cavity of the Pc ring. When CuPcs are deposited on a MoS₂ surface, they form a closely-packed structure with their molecular planes almost parallel to the substrate.^{18–21} Since CuPc has widely-delocalized π -electron orbitals sticking out of the molecular plane, relatively strong tip-sample chemical interactions are expected in NC-AFM imaging of flat-lying CuPcs. In addition, the molecule/substrate interaction forces that anchor the CuPcs to MoS₂ surface are relatively weak¹⁹ so that the molecules are expected to be easily fluctuated by the tip-sample interaction forces. Thus, the organic system is suitable for studies on contrast formation mechanisms in NC-AFM topography and energy dissipation. In this paper, CuPc thin films on MoS₂ surfaces are imaged by NC-AFM with molecular- or even submolecular-scale resolution. Origins of the observed contrasts are discussed in detail. The influence of short-range chemical interactions is particularly considered for the topographic contrasts while the dissipation contrasts are discussed in relation to the structural instabilities in the films.

^{a)}Electronic mail: h-yamada@piezo.kuee.kyoto-u.ac.jp

II. EXPERIMENTAL

The CuPcs (Tokyo Kasei Kogyo Co., Ltd.) were purified by sublimation under vacuum environment ($<10^{-3}$ Pa) before use. The MoS₂ substrates were cleaved in air and annealed at 200 °C for 1 h in an ultrahigh vacuum deposition chamber. The CuPc thin films were prepared by vacuum deposition at a substrate temperature of 100 °C. The vacuum pressure during the deposition was maintained below 10^{-6} Pa. The deposition rate was about 1.5 nm/h, which was monitored by a quartz oscillator. The sample was transferred from the deposition chamber to the AFM chamber without being exposed to the air.

A commercially available NC-AFM apparatus (JEOL: JSPM-4500) with some modifications was used in this experiment. The original frequency shift detector was replaced with a newly developed frequency modulation detector.²² A highly-doped *n*-Si cantilever (Nanosensors: NCH) with a resonance frequency of about 300 kHz and a nominal spring constant of 40 N/m was used for NC-AFM imaging. The *Q*-factor measured under vacuum conditions was about 30,000.

All images shown in this paper were taken under ultrahigh vacuum conditions (base pressure: about 1×10^{-7} Pa) at room temperature. Measurements were performed in the constant frequency shift mode, where the negative shift of the cantilever resonance frequency (Δf) induced by the tip-sample interaction was kept constant during NC-AFM imaging. The cantilever was vibrated at constant amplitude, where the vibration amplitude of the cantilever (*A*) was kept constant by adjusting the amplitude of a cantilever excitation signal (*A_{exc}*). In this excitation mode, energy dissipation caused by the tip-sample interaction can be estimated from the additional increase of *A_{exc}*.²³ Thus, the dissipation image was obtained as a two-dimensional map of *A_{exc}*.

III. RESULTS AND DISCUSSION

A. NC-AFM contrasts

Figures 1(a) and 1(b) are topographic and dissipation images of a CuPc monolayer on the MoS₂ surface, respectively. These images are processed with a tilt compensation filter and a smoothing filter. The topographic image shows individual molecules in the closely-packed structure. On the other hand, the dissipation image shows inverted contrast with respect to the topographic image. Figure 1(c) shows a cross-sectional plot measured along a bright line A–B indicated in Fig. 1(a), revealing the existence of a molecular height variation. The plot shows that the magnitude of height variation is about 0.05 nm. No long-range regularity is confirmed in the molecular height variation.

Figures 2(a) and 2(b) are topographic and dissipation images taken on the same sample, respectively. These images are also processed with a tilt compensation filter and a smoothing filter. The topographic image shows submolecular-scale contrast, revealing the four-leaf structure of the CuPcs. The image also shows an asymmetric feature inside the molecule. The central part of the CuPcs is imaged as an “apparent hole,” which is about 50–60 pm lower than the average molecular plane. The dissipation image also shows a

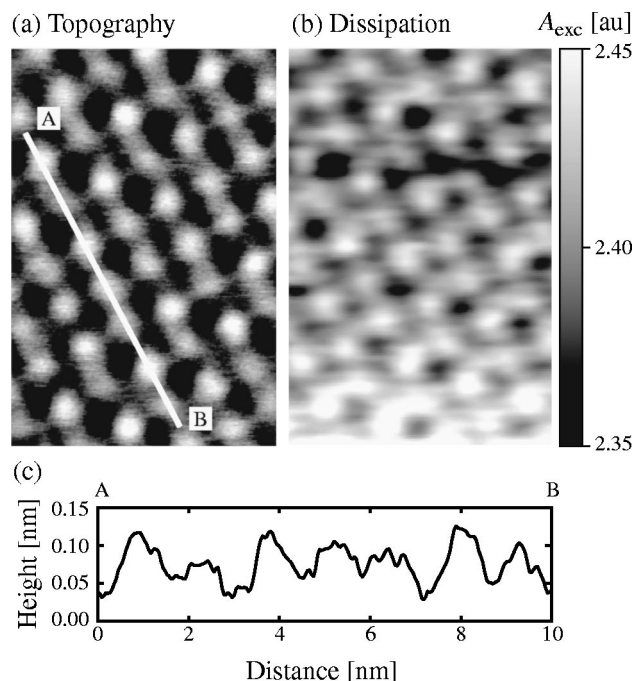


FIG. 1. NC-AFM images of a CuPc monolayer on the MoS₂ surface. (a) Topographic and (b) dissipation images (8 nm×12 nm, $\Delta f = -40$ Hz, *A* = 11 nm_{p-p}). (c) Cross-sectional plot measured along the bright line A–B shown in (a).

submolecular-scale contrast. The asymmetric feature inside the molecule is more evident in the dissipation image than that in the topographic image. The maxima in energy dissipation are located at the inter-molecular spaces as indicated by the white arrows in Fig. 2(a) and 2(b). These submolecular-scale dissipation contrasts are observed even with a relatively fast scanning speed and a relatively large time constant of tip-sample distance regulation. Thus, the contrasts are not likely to be caused by the topographic artifacts. The magnitude of energy dissipation was drastically changed at the lower part of the image, suggesting an atomic-scale tip change.¹⁵

So far, Okudaira *et al.* have studied the molecular tilt angle of CuPcs on the MoS₂ surface using angle-resolved ultraviolet photoelectron spectroscopy (ARUPS).²¹ The ARUPS result showed the best agreement with a molecular tilt angle of 6°, showing that the molecules are not always completely flat-lying on the surface. The asymmetric feature inside the molecules observed in our experiment can be ex-

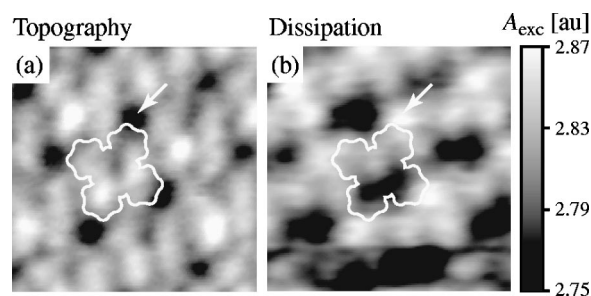


FIG. 2. NC-AFM images of a CuPc monolayer on the MoS₂ surface. (a) Topographic and (b) dissipation images (4 nm×4 nm, $\Delta f = -45$ Hz, *A* = 11 nm_{p-p}).

plained by the inclination of the molecular planes. Since the asymmetry was reproducibly observed even with a different tip, the influence of the tip structure is negligible. There is little possibility of the conformation change of CuPcs because their molecular structure is very stable. The molecular height variations found in the CuPc monolayer [Fig. 1(a)] is probably ascribed to the slight difference in the tilt angles of molecular planes.

Since a copper ion is small enough to be fully accommodated in the central cavity of a Pc ring, CuPc has a completely planar structure. In addition, van der Waals radii for carbon, nitrogen and copper atoms are 170, 155 and 140 pm, respectively. Accordingly, the apparent holes (50–60 pm in depth) found in the NC-AFM image cannot be explained simply by the molecular structure. Such apparent holes have been also found in previously reported STM images of CuPcs on various surfaces such as MoS₂,²⁰ graphite,²⁰ Au(111)^{24,25} and Cu(100).²⁶ The formation mechanism of these STM contrasts has been explained by taking account of spatial distribution of molecular orbitals.^{24–26} CuPc has lower charge densities of highest occupied molecular orbital (HOMO) and least unoccupied molecular orbital (LUMO) at the center of the molecule.²⁶ Thus, the strong dependence of tunneling probability on HOMO and LUMO densities leads STM images to represent not only the geometrical structure but also the electronic structure of CuPcs.

As for NC-AFM, recent studies on inorganic surfaces such as Si(111) suggested that the short-range chemical interaction between a tip front atom and a surface atom plays an important role in the formation of atomic-scale NC-AFM contrasts.²⁷ Similarly, even in the case of organic surfaces, we expect that the short-range chemical interactions should be important. In general, frontier orbitals such as HOMO and LUMO are chemically more reactive than other molecular orbitals. Hence, the apparent holes found in the NC-AFM image may reflect the spatial distribution of the frontier orbitals.

One of the possible explanations for the large dissipation at the inter-molecular spaces is described as follows. When a tip is located just on top of a molecule, the molecule will be fluctuated by the tip-sample interaction. Then the kinetic energy of the molecular fluctuation will be dissipated through the surrounding molecules and the substrate due to a stochastic dissipation process. Moreover, when a tip is positioned just over the inter-molecular space indicated by white arrows in Figs. 2(a) and 2(b), four adjacent molecules will be involved with the dissipation process, leading to the largest energy dissipation. Thus, the molecular-scale dissipation contrasts are probably related to the number of the molecules interacting with the tip. This interpretation also applies to the molecular-scale dissipation contrast in Fig. 1(b), where the dissipation image exhibits an inverted contrast with respect to the corresponding topographic contrast.

B. Monolayer and multilayer

Multilayer domains of CuPc were formed with a longer deposition time (1 h) compared to the case of monolayer formation (10-minute deposition). Figures 3(a) and 3(b) are

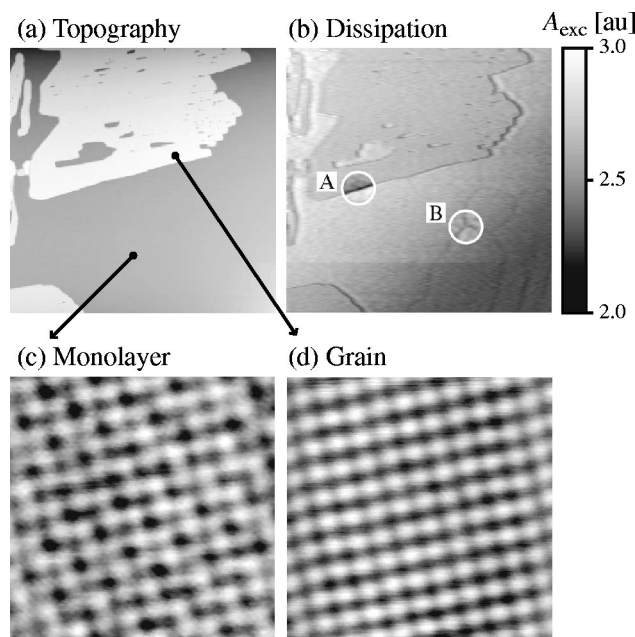


FIG. 3. (a) Topographic and (b) dissipation images of a CuPc thin film on MoS₂ surface ($2\ \mu\text{m} \times 2\ \mu\text{m}$, $\Delta f = -25\ \text{Hz}$, $A = 12.5\ \text{nm}_{p-p}$). The MoS₂ surface was completely covered with a CuPc monolayer. Then the micrometer-scale grains are formed on top of the monolayer. Molecularly-resolved NC-AFM images were taken on both (c) the monolayer and (d) the grain ($15\ \text{nm} \times 15\ \text{nm}$, $\Delta f = -30\ \text{Hz}$, $A = 14\ \text{nm}_{p-p}$).

topographic and dissipation images taken on the sample, showing some micrometer-scale grains. The height of these grains estimated from a cross-sectional plot of the topographic image is about 10 nm, which corresponds to the thickness of about 30 molecular layers. The scanned area of the images is so large ($2\ \mu\text{m} \times 2\ \mu\text{m}$) that the effect of substrate inclination cannot be neglected. In this experiment, the tip-sample distance regulation was made by a simple proportional feedback control so that the steady-state error was not completely excluded. The corresponding dissipation image [Fig. 3(b)] also shows the effect of the substrate inclination and hence the contrast is not clear enough to show important features. Thus, the regions surrounded by white circles A and B are shown with enhanced contrasts. The dissipation contrast in circle A reveals that the energy dissipation on the grain is lower than that on the monolayer. In addition, some dark lines are found in circle B.

Figures 3(c) and 3(d) are molecularly-resolved NC-AFM images taken on the monolayer and the grain, respectively, as indicated by the black arrows in Fig. 3. Since STM imaging of CuPc multilayers is difficult due to their poor electrical conductivities, molecular-scale investigations of the surface structure has not been performed. Thus, the NC-AFM image shown in Fig. 3 has first revealed the molecular-scale surface structure of a CuPc multilayer. The NC-AFM images reveal that the grain surface has basically the same structure as that of the monolayer. However, a remarkable difference is found in the structural uniformity. The grain surface showed much better uniformity of the molecular height than the monolayer surface. As pointed out in the discussion on Fig. 1, the molecular height variation is probably due to the difference in the molecular tilt angles. The result suggests that the increas-

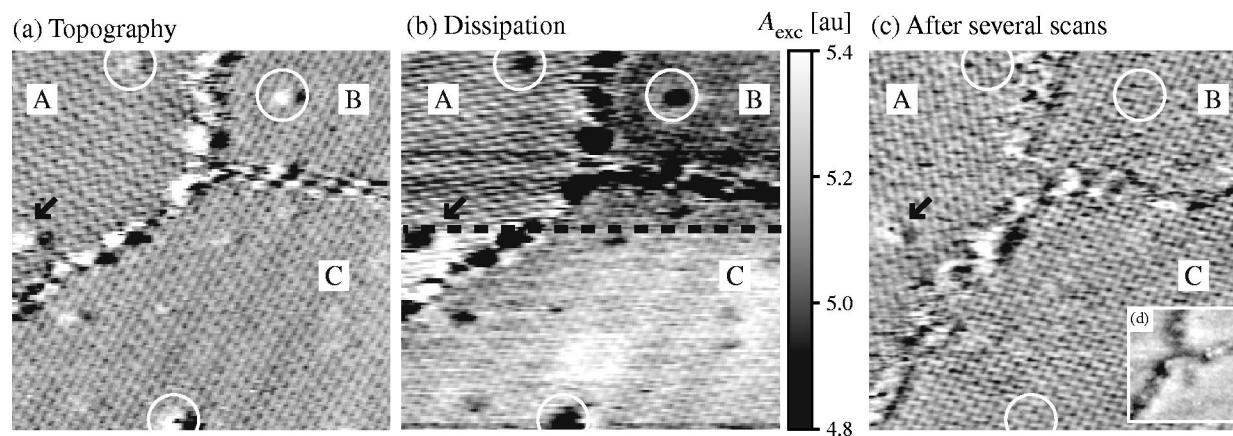


FIG. 4. (a) Topographic and (b) dissipation images of a CuPc monolayer on MoS₂ surface (50 nm×50 nm, $\Delta f = -50$ Hz, $A = 14$ nm_{p-p}). (c) The NC-AFM image taken on the same area after several scans (50 nm×50 nm, $\Delta f = -55$ Hz, $A = 12.5$ nm_{p-p}). (d) The NC-AFM image taken on the same area with a much smaller frequency shift (50 nm×50 nm, $\Delta f = -5$ Hz, $A = 11$ nm_{p-p}).

ing thickness reduces the influence from the film/substrate interaction, which allow CuPcs to take an well-ordered structure.

This structural difference between the monolayer and the multilayer can explain the dissipation contrast at the monolayer/grain boundary [circle A in Fig. 3(b)]. The observed molecular height variation suggests that CuPcs in the monolayer were loosely bound by the neighboring molecules and the MoS₂ surface. Such a loosely bound molecule can be easily fluctuated by the tip-sample interaction, yielding a larger energy dissipation. On the other hand, the excellent structural uniformity of the grain surface implies that the molecules on the grain are more tightly bound by the neighboring molecules. In addition, they may be stabilized by the crystalline field of the large grain. Such a tightly bound molecule should be structurally stable against the tip-sample interaction, resulting in a smaller energy dissipation. These results suggest that the strong correlation between molecular fluctuations and energy dissipation allows us to study the structural stability of a surface from dissipation contrasts.

C. Domain boundaries

Figures 4(a) and 4(b) show topographic and dissipation images, respectively, taken on the area indicated by white circle B in Fig. 3(b). These images reveal that the dark lines found in the dissipation image shown in Fig. 3(b) correspond to the boundaries of monolayer domains A, B and C. The topographic image [Fig. 4(a)] reveals that domain A is different in orientation from domains B and C. The dissipation image [Fig. 4(b)] shows that energy dissipation measured on some defects and the domain boundaries is smaller than that on the monolayer. The energy dissipation values measured on domains B and C are slightly smaller than that on domain A, suggesting that the energy dissipation is dependent on the orientation of molecular packing arrangements with respect to the tip. Such a strong dependence of energy dissipation on tip geometry is also confirmed by a drastic contrast change in the dissipation image shown in Fig. 4(b) as indicated by a dotted line. This is probably due to an atomic-scale tip change.¹⁵ Figure 4(c) shows the NC-AFM image taken on

the same area after several scans. The image reveals that the molecular arrangement at the domain boundaries were improved and some defects indicated by white circles disappeared during the NC-AFM imaging. Note that a black arrow in each of Figs. 4(a)–4(c) indicates the same defect that can identify the relative position of the image. Figure 4(d), which is shown as an inset in Fig. 4(c), is an NC-AFM image taken on the same area with a much smaller frequency shift (–5 Hz). The image shows an inverted contrast at the domain boundaries with respect to the image shown in Fig. 4(c).

The energy dissipation measured on the domain boundaries and film defects are smaller than that on the monolayer. Thus, the energy dissipation changes when a tip is scanned over these areas. When a tip is scanned with a relatively small frequency shift [e.g., Fig. 4(d)], the dissipation change is relatively small so that the amplitude regulation can respond quickly enough to suppress the transient response of the tip-sample distance regulation feedback that can induce topographic artifacts. With an increase in the frequency shift, however, the dissipation change becomes so large that the time response of the amplitude feedback regulation becomes insufficient to prevent the topographic artifacts [e.g., Fig. 4(c)]. Accordingly, the topographic image shown in Fig. 4(d) more accurately represents the real surface structures than the image shown in Fig. 4(c). The topographic image shown in Fig. 4(d) reveals that the domain boundaries and defects correspond to the absence of molecules. This result can explain the smaller energy dissipation at these areas because the number of molecules interacting with a tip is smaller than that on the monolayer.

The mechanism for the observed tip-induced surface modification can be understood from the analogy to the annealing effect. In general, molecular ordering is often improved by annealing treatment. This is because such a heating treatment gives molecules some extra energy to break up an original packing arrangement to form a well-ordered structure with a lower free energy. In this experiment, molecules were given extra energy through the dissipative tip-sample interaction. In that sense, the surface modification

can be regarded as “local annealing” induced by the tip-sample interaction. Furthermore, this result is direct evidence which confirms that some of the vibration energy of the cantilever was transformed into the kinetic energy of molecular fluctuations through dissipative tip-sample interactions.

IV. CONCLUSIONS

In this study, we have investigated CuPc thin films deposited on MoS₂ surfaces by NC-AFM. Submolecular resolution was successfully obtained in both topographic and dissipation images of CuPc monolayers. The topographic contrasts suggest the effect of tip-sample chemical interactions while the dissipation contrasts show close correlation with the number of molecules interacting with a tip. A molecularly-resolved NC-AFM image was also obtained on the CuPc multilayer, revealing that the multilayer surface has much better uniformity in molecular tilt angle than monolayer surface. The energy dissipation measured on the multilayer was smaller than that on the monolayer, reflecting the difference in structural stabilities against tip-sample interactions. A local surface modification of a CuPc monolayer was demonstrated by NC-AFM. This is a direct evidence for the existence of energy transfer from the vibrating cantilever to the molecules through dissipative tip-sample interactions. Although the surface modification was not performed in an well-controlled manner, the result presents the promising aspects of NC-AFM for the future applications to controlled molecular manipulation.

ACKNOWLEDGMENTS

The support of Kyoto University Venture Business Laboratory (KU-VBL), a Grant-in-Aid from the Ministry of Education, Science, Sports and Culture of Japan, and Research Fellowships of the Japan Society for the Promotion of Science for Young Scientists are gratefully acknowledged.

¹T. R. Albrecht, P. Grütter, D. Horne, and D. Rugar, *J. Appl. Phys.* **69**, 668 (1991).

²M. Bammerlin, R. Lüthi, E. Meyer, A. Baratoff, J. Lü, M. Guggisberg, C. Gerber, L. Howald, and H.-J. Güntherodt, *Probe Microsc.* **1**, 3 (1997).

³F. J. Giessibl, *Science* **267**, 68 (1995).

⁴S. Kitamura and M. Iwatsuki, *Jpn. J. Appl. Phys., Part 2* **34**, L1086 (1995).

⁵K. Kobayashi, H. Yamada, T. Horiuchi, and K. Matsushige, *Appl. Surf. Sci.* **140**, 281 (1999).

⁶K. Kobayashi, H. Yamada, T. Horiuchi, and K. Matsushige, *Jpn. J. Appl. Phys., Part 2* **38**, L1550 (1999).

⁷T. Fukuma, K. Kobayashi, T. Horiuchi, H. Yamada, and K. Matsushige, *Appl. Phys. A: Mater. Sci. Process.* **72**, S109 (2001).

⁸T. Fukuma, K. Kobayashi, K. Noda, K. Ishida, T. Horiuchi, H. Yamada, and K. Matsushige, *Surf. Sci.* **516**, 103 (2002).

⁹A. I. Livshits, A. L. Shluger, A. L. Rohl, and A. S. Foster, *Phys. Rev. B* **59**, 2436 (1999).

¹⁰S. H. Ke, T. Uda, R. Pérez, I. Štich, and K. Terakura, *Phys. Rev. B* **60**, 11631 (1999).

¹¹N. Sasaki and M. Tsukada, *Jpn. J. Appl. Phys.* **39**, L1334 (2000).

¹²T. Uchihashi, T. Okada, Y. Sugawara, K. Yokoyama, and S. Morita, *Phys. Rev. B* **60**, 8309 (1999).

¹³T. Uchihashi, Y. Sugawara, T. Tsukamoto, T. Minobe, S. Orisaka, T. Okada, and S. Morita, *Appl. Surf. Sci.* **140**, 304 (1999).

¹⁴R. Lüthi, E. Meyer, M. Bammerlin, A. Baratoff, L. Howald, C. Gerber, and H.-J. Güntherodt, *Surf. Rev. Lett.* **4**, 1025 (1997).

¹⁵R. Bennewitz, A. S. Foster, L. N. Kantrovich, M. Bammerlin, C. Loppacher, S. Schär, M. Guggisberg, and E. Meyer, *Phys. Rev. B* **62**, 2074 (2000).

¹⁶C. Loppacher, R. Bennewitz, O. Pfeiffer, M. Guggisberg, M. Bammerlin, S. Schär, V. Barwich, A. Baratoff, and E. Meyer, *Phys. Rev. B* **62**, 13674 (2000).

¹⁷M. Gauthier and M. Tsukada, *Phys. Rev. B* **60**, 11716 (1999).

¹⁸M. Hara, H. Sasabe, A. Yamada, and A. F. Garito, *Jpn. J. Appl. Phys., Part 2* **28**, L306 (1989).

¹⁹C. D. England, C. E. Collins, T. J. Schuerlein, and N. R. Armstrong, *Langmuir* **10**, 2748 (1994).

²⁰C. Ludwig, R. Strohmaier, J. Petersen, B. Gompf, and W. Eisenmenger, *J. Vac. Sci. Technol. B* **12**, 1963 (1994).

²¹K. K. Okudaira, S. Hasegawa, H. Ishii, K. Seki, Y. Harada, and N. Ueno, *J. Appl. Phys.* **85**, 6453 (1999).

²²K. Kobayashi, H. Yamada, H. Itoh, T. Horiuchi, and K. Matsushige, *Rev. Sci. Instrum.* **72**, 4383 (2001).

²³B. Gotsmann, C. Seidel, B. Anczykowski, and H. Fuchs, *Phys. Rev. B* **60**, 11051 (1999).

²⁴X. Lu, K. W. Hipps, X. D. Wang, and U. Mazur, *J. Am. Chem. Soc.* **118**, 7197 (1996).

²⁵K. W. Hipps, X. Lu, X. D. Wang, and U. Mazur, *J. Phys. Chem.* **100**, 11207 (1996).

²⁶P. H. Lippel, R. J. Wilson, M. D. Miller, C. Wöll, and S. Chiang, *Phys. Rev. Lett.* **62**, 171 (1989).

²⁷S. Morita, R. Wiesendanger, and E. Meyer, in *Noncontact Atomic Force Microscopy (Nanoscience and Technology)* (Springer-Verlag, Berlin, 2002).